Spectroscopic Characteristics of Rhodamine B Dye inside Tin Dioxide Thin Film-Coated Cavity

Durayd M. Kassim, Thiaa H. Sahoon

Department of Electronic Engineering, Middel Technical University, Najaf, IRAQ

Abstract

In this work, nanostructured tin dioxide films were deposited by closed-field unbalanced dc magnetron sputtering technique on two sides of quartz cells containing Rhodamine B dye dissolved in ethanol with 10^{-5} M concentration. The preparation conditions were optimized to prepare highly pure SnO_2 nanostructures with a minimum particle size of about 20nm. The effect of SnO_2 films as external cavity for the random gain medium was determined by the laser-induced fluorescence of this medium and an increase of about 200% in intensity was observed after the deposition of nanostructured SnO_2 thin films on two sides of the dye cell.

Keywords: Nanostructures; Tin dioxide; Spectroscopic characteristics; Magnetron sputtering
Received: 19 October 2023; **Revised:** 09 December; **Accepted:** 16 December; **Published:** 1 January 2024

1. Introduction

Improving the active medium of the dye laser has attracted the interest of many researches and studies. The first attempts started in the 1960 and continued up to now. It involves using polymer solutions that include organic dyes to form laser dye active media [1-2]. The dyes, used as a host of the active media, are generally in the liquid phase. The control over such active medium in this state is very difficult and it has many disadvantages [3,4]. Therefore, many researches have been done to incorporate it into a solid host, such as polymers glass, to obtain a solid active medium [5-8].

Rhodamine B (RB) dye is considered as a common typical material that belongs to the xanthene group and operates in the visible range [9-11]. The lasing emission of RB dye is also dependent on the type of solvent used for dissolving this dye to form its solution [12,13]. For example, the central lasing wavelength is increased by about 43nm when changing the solvent from ethanol to ethylene glycol [14]. In general, the lasing emission is ranging within 570-682nm [15,16].

The unique properties of this dye have attracted the attention of researchers in several military, medical, and industrial applications as it will be illustrated in the random laser application section [17,18]. The fluorescence lifetime of this dye is about (4.08×10^{-9}s), which means that the possibility of inter-system crossing is very weak ($<10^{7}$ s^{-1}) [19]. Using rhodamine dye as an active media of dye laser, it is possible to obtain continuous or pulsed laser output according to the pumping method in which a wide tunable wavelengths range can be obtained [20-22].

In this work, nanostructured silicon dioxide films are deposited by closed-field unbalanced dc magnetron sputtering technique on two sides of quartz cells containing Rhodamine B dye dissolved in ethanol with 10^{-5} M concentration as a random gain medium. The preparation conditions are optimized to prepare highly pure SnO_2 nanostructures with as minimum as possible particle size. The effect of SnO_2 films as external cavity for the random gain medium is studied by the laser-induced fluorescence of this medium.

2. Experimental Part

A tin sheet of 10cm in diameter and 300μm in thickness was used as the target to be sputtered and maintained carefully on the cathode. It was cleaned by HF acid, ethanol and distilled water, dried and then used for deposition process. Highly-pure argon and oxygen gases were used as discharge and reactive gases, respectively. The deposition

process was performed on quartz cells. Before using them in sputtering experiments, these cells were first cleaned with ethanol to remove any oil layers or residuals may exist on their surfaces, rinsed and washed with distilled water to remove ethanol, and then dried completely before being kept in clean case or placed inside vacuum chamber. More details on the deposition system can be found in previous works [23-26].

The Rhodamine B laser dye solutions were prepared by dissolving the required amount of the dye in the solvents (ethanol, acetone, chloroform or ethylene glycol). This amount of the dye (W) was weighed using a precise digital balance of 10^{-4}g sensitivity (Matter Company) and can be calculated using the following equation [24]:

$$W = \frac{M_W.V.C}{1000} \quad (1)$$

where M_w is the molecular weight of the dye (g/mole), V is the volume of the solvent (ml) and C is the molar concentration (mole/liter)

A high concentration of 10^{-2} mole/liter of RB dye solutions was prepared and then diluted to different concentrations of 10^{-3}, $5x10^{-3}$, 10^{-4}, $5x10^{-4}$, 10^{-5}, $5x10^{-5}$ and 10^{-6} mole/liter.

The operating conditions of the system were divided into two groups; constant and variable. The constant operating conditions include vacuum pressure, current limiting resistance, discharge voltage, discharge current, cooling temperature, cooling water flow rate and deposition time. The variable operating conditions include gas pressure, inter-electrode distance, gas mixing ration and gas flow rate. Varying discharge voltage was almost possible during the operation. In addition, turning the cooling system off would raise the temperature of either electrode to 40-45°C with circulating water, while stopping the circulation of water would raise electrode temperature more (up to 150°C).

The quartz cell to be coated is located where completely immersed in the generated plasma. Big efforts were made to obtain uniform spatial distribution of plasma column in order to ensure homogeneous growth of prepared films. This could be done by controlling operation conditions and parameters, mainly the inter-electrode distance, gas flow and discharge current.

The samples prepared in this work were characterized in order to determine their structural and spectral characteristics. Transmission and absorption spectra of the prepared samples were recorded in the spectral range 200-800nm with an optical resolution of about 0.2nm by using a UV-Visible spectrophotometer (K-MAC SpectraAcademy SV-2100). The fluorescence spectra were recorded using F96 fluorescence spectrophotometer (Shanghai LengGuang Tech. Co., Ltd.) in the emission wavelengths range 180-900nm, with xenon CW lamp as the excitation source.

The optimum conditions to prepare tin dioxide nano films on the external walls of the quartz cell are inter-electrode distance of 4cm, Ar:O_2 gas mixing ratio of 70:30, total gas pressure of 0.08torr, discharge voltage of 2.5kV, discharge current of 35mA, anode temperature of 27°C (room temperature) and cathode temperature of about 40°C.

3. Results and Discussion

The fluorescence was measured for the RB dye in the quartz cells, as shown in Fig. (1), before and after deposition of nanostructured SnO_2 thin films on two sides of these cells. It is clear that the optimum molar concentration of Rhodamine B dye dissolved in ethanol is 10^{-5} M as the highest intensity was recorded. It looks that the behavior of Rhodamine B dye dissolved in ethanol is very dependent on the dye concentration.

Certain applications of nanostructures, such as photodetectors, energy conversion devices, gas sensing and ultra-hard coatings, require as high as possible surface area. Therefore, the prepared samples can be efficiently used for such applications [27-29].

In order to introduce the effect of nanostructured SnO_2 thin films deposited on two sides of the dye cell on the fluorescence

of the dye medium, and hence on the gain characteristics, the fluorescence was recorded for the dye sample before and after the deposition of SnO_2 films for RB dye, as shown in Fig. (9) at certain concentration of 10^{-5} M. As the SnO_2 film thickness is decreased with decreasing deposition time, the particle density is decreased too. Accordingly, the role of the deposited SnO_2 films as an external cavity, and hence the increase in the medium gain, is decreased. However, working at long deposition time may lead to growth of large particles and then more agglomeration over the film surface.

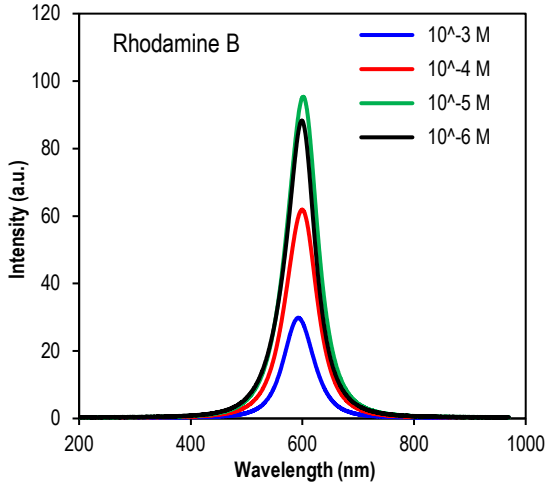

Fig. (1) Fluorescence spectra of Rhodamine B dye dissolved in ethanol recorded at different concentrations

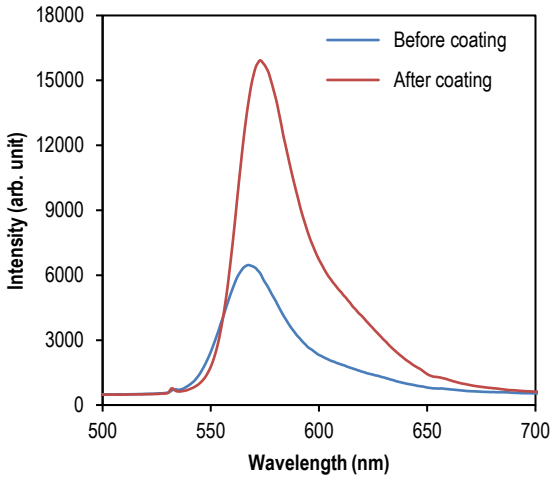

Fig. (9) Laser-induced fluorescence of Rhodamine B dye before and after the deposition of nanostructured SnO_2 thin films on two sides of the dye cell

4. Conclusion

In concluding remarks, highly-pure nanostructured tin dioxide films with particle size of 20nm deposited by closed-field unbalanced dc magnetron sputtering technique on two sides of quartz cells containing Rhodamine B dye dissolved in ethanol with 10^{-5} M concentration act as external cavity for this random gain medium. This role was determined by the laser-induced fluorescence of the dye sample and an increase of about 200% in intensity was observed after the deposition of nanostructured SnO_2 thin films.

References

[1] A. Ranjgar et al., "Characterization and Optical Absorption Properties of Plasmonic Nanostructured Thin Films", Armenian J. Phys., 6(4) (2013) 198-203.

[2] O.A. Hamadi, "Characteristics of CdO-Si heterostructure produced by plasma-induced bonding technique," Proc. IMechE Part L: J. Mater. Design and Applications, 222, 2008, 65–71.

[3] A. Tabata et al., "Optical properties and structure of SiO_2 films prepared by ion-beam sputtering", Thin Solid Films, 289 (1996) 84-89.

[4] A.K. Yousif and O.A. Hamadi, "Plasma-induced etching of silicon surfaces," Bulg. J. Phys., 35(3) (2008) 191–197.

[5] A.M. Al-Dhafiri, "High-Quality Plasma-Induced Crystallization of Amorphous Silicon Structures", Iraqi J. Appl. Phys., 5(1) (2009) 35-39.

[6] Hammadi OA. Effects of Extraction Parameters on Particle Size of Titanium Dioxide Nanopowders Prepared by Physical Vapor Deposition Technique, Plasmonics, 15 (2020) 1747-1754.

[7] A.T.S. Yee, "Synthesis of Silicon Nanowires by Selective Etching Process", Iraqi J. Appl. Phys., 4(3) (2008) 15-17.

[8] Bang SB, Chung TH, Kim Y, Kang MS, Kim JK, "Effects of the oxygen fraction and substrate bias power on the electrical and optical properties of silicon oxide films by plasma enhanced chemical vapour deposition using TMOS/O_2 gas", J. Phys. D: Appl. Phys., 37 (2004) 1679-1684.

[9] E.S.M. Goh, T.P. Chen, C.Q. Sun and Y.C. Liu, "Thickness effect on the band gap and optical properties of germanium thin films", J. Appl. Phys., 107 (2010) 024305.

[10] O.A. Hammadi, "Characteristics of Heat-Annealed Silicon Homojunction Infrared

Photodetector Fabricated by Plasma-Assisted Technique", Phot. Sens., 6(4) (2016) 345-350.
[11] H. Jung, W.H. Kim, I.K. Oh, C.W. Lee, C. Lansalot-Matras, S.J. Lee, J.M. Myoung, H.B. Ram Lee and H. Kim, "Growth characteristics and electrical properties of SiO_2 thin films prepared using plasma-enhanced atomic layer deposition and chemical vapor deposition with an aminosilane precursor", J. Mater. Sci., 51(11) (2016) 5082-5091.
[12] O.A. Hammadi, "Characterization of SiC/Si Heterojunction Fabricated by Plasma-Induced Growth of Nanostructured Silicon Carbide Layer on Silicon Surface", Iraqi J. Appl. Phys., 12(2) (2016) 9-13.
[13] D. Hiller et al., "Low temperature silicon dioxide by thermal atomic layer deposition: investigation of material properties", J. Appl. Phys., 107 (2010) 064314-1–064314-10.
[14] Y. Inoue and O. Takai, "Spectroscopic studies on preparation of silicon oxide films by PECVD using organosilicon compounds", Plasma Sources Sci. Technol., 5 (1996) 339-343.
[15] O.A. Hammadi, "Photovoltaic properties of thermally-grown selenium-doped silicon photodiodes for infrared detection applications," Phot. Sens., 5(2) (2015) 152–158.
[16] S. Kamiyama, T. Miura and Y. Nara, "Comparison between SiO_2 films deposited by atomic layer deposition with $SiH_2[N(CH_3)_2]_2$ and $SiH[N(CH_3)_2]_3$ precursors", Thin Solid Films, 515 (2006) 1517-1521.
[17] J.W. Klaus et al., "Atomic layer controlled growth of SiO_2 films using binary reaction sequence chemistry", Appl. Phys. Lett., 70 (1997) 1092–1094.
[18] J.-H. Lee et al., "Investigation of silicon oxide thin films prepared by atomic layer deposition using SiH_2Cl_2 and O_3 as the precursors", Jpn. J. Appl. Phys., 43 (2004) L328–L330.
[19] O.A. Hamadi, "Effect of annealing on the electrical characteristics of CdO-Si heterostructure produced by plasma-induced bonding technique," Iraqi J. Appl. Phys., 4(3) (2008) 34–37.
[20] O.A. Hammadi, M.K. Khalaf and F.J. Kadhim, "Fabrication and characterization of UV photodetectors based on silicon nitride nanostructures prepared by magnetron sputtering," Proc. IMechE Part N: J. Nanoeng. Nanosys., 230(1) (2015) 32–36.
[21] O.A. Hammadi, M.K. Khalaf and F.J. Kadhim, "Fabrication of UV photodetector from nickel oxide nanoparticles deposited on silicon substrate by closed-field unbalanced dual magnetron sputtering techniques," Opt. Quantum Electron., 47(2) (2015) 1–9.
[22] P. Pan, "The composition and properties of PECVD silicon oxide films", J. Electrochem. Soc., 132 (1985) 2012–2019.
[23] O.A. Hammadi, M.K. Khalaf, F.J. Kadhim and B.T. Chiad, "Operation characteristics of a closed-field unbalanced dual-magnetrons plasma sputtering system," Bulg. J. Phys., 41(1) (2014) 24–33.
[24] T. Tamura et al., "First-principles analysis of optical absorption edge in pure and fluorine-doped SiO_2 glass", Comput. Mater. Sci., 44 (2008) 61-66.
[25] W.F. Wu and B.S. Chiou, "Optical and mechanical properties of reactively sputtered silicon dioxide films", Semicond. Sci. Technol. 11 (1996) 1317-1321.
[26] Hammadi OA, Khalaf MK and Kadhim FJ. Fabrication of UV Photodetector from Nickel Oxide Nanoparticles Deposited on Silicon Substrate by Closed-Field Unbalanced Dual Magnetron Sputtering Techniques. Opt Quantum Electron, 47 (2015) 3805-3813.
[27] Hammadi OA, Khalaf MK and Kadhim FJ. Fabrication and Characterization of UV Photodetectors Based on Silicon Nitride Nanostructures Prepared by Magnetron Sputtering. Proc IMechE Part N, J Nanoeng Nanosys, 230 (2016) 32-36.
[28] Hammadi OA, Al-Maliki FJ and Al-Oubidy EA. Photocatalytic Activity of Nitrogen-Doped Titanium Dioxide Nanostructures Synthesized by DC Reactive Magnetron Sputtering Technique. Nonl Opt Quantum Opt, 51 (2019) 67-78.

